Int. J. Electrochem. Sci., 11 **(2016)** 5353 – 5363, doi: 10.20964/2016.07.33

International Journal of
ELECTROCHEMICAL
SCIENCE
www.electrochemsci.org

Supercapacitive Properties of Activated Carbon-Quinone Derivative Composite Electrode in Different Hydrogen ion Conducting Electrolytes

Mohammed Latifatu[1], *Hae Soo Lee, Choog Sup Yoon*[2], *Jemyung Oh*[3], *Jeong Ho Park*[1,*], *Jang Woo Park, Jang Myoun Ko*[1,*]

[1] Department of Chemical and Biological Engineering, Hanbat National University, Daejon 305-719, South Korea
[2] Advanced Materials, Hanbat National University, Daejon 34158, Repubic of Korea
[3] Materials Engineering Department, Adama Science and Technology University, Ethiopia
[*]E-mail: jmko@hanbat.ac.kr, jhpark@hanbat.ac.kr

Received: 24 February 2016 / *Accepted:* 18 March 2016 / *Published:* 4 June 2016

A composite electrode (CE) consisting of activated carbon and quinine derivative 2-((2-(1*H*-indol-3-yl) ethyl) amino) naphthalene-1, 4-dione (HBU-551) was probed in different hydrogen ion conducting electrolytes such as sulfuric acid (H_2SO_4), hydrochloric acid (HCl), Phosphoric acid (H_3PO_4) and ammonium chloride (NH_4Cl). The electrochemical performances of the CE in the electrolytes were investigated by cyclic voltammetry (CV), electrochemical impedance spectroscopy (EIS) and charge-discharge. The different hydrogen ion conducting electrolytes with different ionic conductivity induce different electrochemical properties in the CE. The specific capacitance is in the order of H_2SO_4 > H_3PO_4 > HCL > NH_4Cl at 100 mV/s and a potential range of -0.2 - 0.8 (V vs Ag/AgCl).

Keywords: Quinone derivative, composite electrode, proton conducting electrolyte, supercapacitor

1. INTRODUCTION

Electrochemical capacitors are applicable in several systems such as laptop computers, cellular phones, and hybrid electric vehicles [1-2]. Quinone-based materials have attracted considerable attention as electrode materials for energy storage devices including electrochemical capacitors [3, 4], lithium-ion batteries [5, 6], redox flow batteries [7], and polymer/air batteries [8]. They are promising organic material for electrochemical cells because they are cost effective, environmentally friendly and exhibit high reversibility [9]. The next important component of the electrochemical cell besides the electrode material is the electrolyte. The electrolyte determines the internal resistance and power

capability of the electrochemical cell. Aqueous electrolytes have often been used as electrolytes for supercapacitors due to their high ionic conductivity, low resistance, their compatibility with electrodes, low cost and environmental friendliness. Proton conducting electrolytes have attracted attention over the years due to the small radius of proton (H^+) compared to other ions [10]. Among these, H_2SO_4, H_3PO_4 and HCl have extensively been used for supercapacitor fabrication [11-13]. Hydrogen-bonding and protonation are the basic factors influencing the potentials and mechanisms in the redox behavior of quinones [14]. In acidic, neutral, and alkaline solutions, quinone based compounds undergo reversible two-electron reduction reaction. In acidic medium, the reduction is a single step two-electron, two-proton process. In alkaline solution, the reaction does not involve proton but includes two-electron reduction process. In neutral medium, the reduction involves one proton two-electron or only two electrons without the contribution of proton [15-17]. Scheme 1a shows the redox reaction of quinone (Q)-hydroquinone (QH2) couple in acidic medium ($[H^+] > [Q]$). [17].

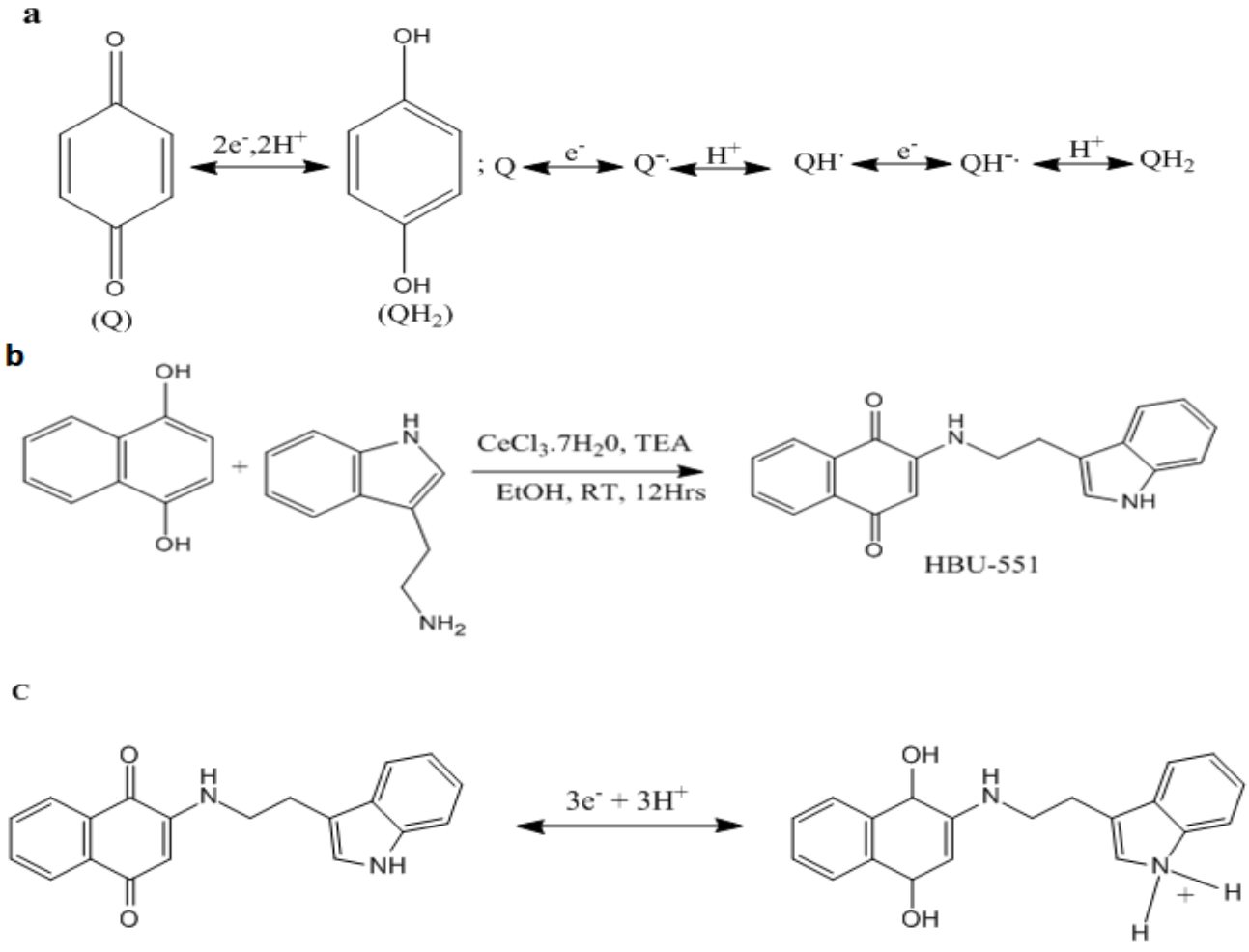

Scheme 1. (a) The redox reaction of quinone (Q)-hydroquinone (QH_2) couple in acidic medium ($[H^+] > [Q]$). (b) Synthesis reaction of the HBU-551 from 2, 3-dihydro-1, 4-naphthoquinone and trypt amine; (c) propose redox reaction mechanism of the HBU-551

In this study, 1, 4-dihydoxynapthalene derivatives HBU-551 was synthesized chemically and physically mixed with porous activated carbon. The electrochemical properties of the CE were probed in different proton conducting electrolyte.

2. EXPERIMENTAL

2.1. Synthesis of HBU-551

1, 4-Dihydrxy naphthalene (100 mg, 0.62 mmol) was dissolved in EtOH (10 mL). Cerium chloride (20 mg, 0.06 mmol) and tryptamine (120 mg, 0.75 mmol) were added to the solution. Finally, the TEA (0.18 mL, 1.25 mmol) was added. The reaction mixture was stirred at room temperature for 12hrs. After that, the reaction mixture was poured into 20 mL crushed ice with constant stirring. The solid was filtered, washed with H_2O, and then dried under a vacuum. The HBU-551 was obtained (160mg, 85.04%). Scheme 1b shows the synthetic reaction of the HBU-551. The structure of HBU-551 was elucidated using a 1H nuclear magnetic resonance (1H NMR) spectroscopy (Varian Gemini 200 NMR), which was identified as follows: ^{1}H NMR (400 MHz, DMSO) 3.03(t, *J*=7.6, 2H), 3.48(q, *J*=6.8, 2H), 5.75(s, 1H), 6.99(t, *J*=7.6, 1H), 7.07(t, *J*=7.6, 1H), 7.26(s, 1H), 7.34(d, *J*=8, 1H), 7.53(t, *J*=6, 1H), 7.57(d, *J*=8, 1H), 7.72(td, *J*=7.6, *J*=1.2, 1H), 7.83(td, *J*=7.6, *J*=1.2, 1H), 7.94(dd, *J*=7.6, *J*=1.2, 1H), 7.97(dd, *J*=7.6, *J*=1.2, 1H), 10.87(s, 1H).

2.2. Preparation of the CE

To use the obtained HBU-551 as an electroactive additive for supercapacitor electrodes, the viscous slurry was prepared by mixing activated carbon (MSC-30, specific surface area of 3000 m^2g^{-1}, Kansai Cokes, 70 wt. %) as an active material, the HBU-551 (25 wt. %) synthesized as a redox active additive, and poly(vinylidene fluoride) (Aldrich, 5 wt.%) as a polymeric binder with N-methyl-2-pyrrolidinone as a dispersion solvent. This was done at ambient temperature for 3 hrs. The CE was fabricated by coating the slurry on a platinum current collector (1.0 cm x1.0 cm) and then dried at 100 ^oC in an oven to evaporate the solvent. The loading density of the CE without the platinum is evaluated to be about 2.0 mg/cm^2. For comparison, an activated carbon electrode was also prepared by the same manner without the HBU-551.

2.3. Characterization of the composite powder and CE

The HBU-551, activated carbon, and the composite powders were characterized using a Fourier-transform infrared spectroscopy (Bomem MB100). The surface morphologies of the fabricated electrodes were observed using a field emission scanning electron microscope (Hitachi S-4800).

2.4. Electrochemical measurements

The ionic conductivities of the electrolytes were determined using electrochemical impedance spectroscopy (EIS) Autolab instrument (PGstat 100, Eco Chemie) (FRA software) using a sample cell made of Ni/liquid electrolyte/Ni, in a frequency range of 10^{-2}–10^{5} Hz at ambient temperature. EIS is an indirect procedure for calculating conductivity of materials by fitting the equivalent circuit to the results of measurement. The measurements were recorded at open circuit potential. The resistive behavior of the CE was also subjected to electrochemical impedance spectroscopy performed using the same instrument and the same frequency range with a stimulus potential of 0.5 V. The cyclic voltammetry measurement was conducted in a three-electrode cell, which was equipped with a reference electrode made of Ag/AgCl saturated with KCl, platinum as a counter electrode, and the CE as the working electrode in an aqueous electrolyte solution of 1 M H_2SO_4, 1 M H_3PO_4, 1 M HCl and 1 M NH_4Cl using an Autolab instrument (PGstat 100, Eco Chemie) at different scan rates of 100~1000 mV/s and a potential range of -0.2 to 0.8 V vs. Ag/AgCl. The specific capacitance (C) was calculated as a function of scan rate using the equation:

$$C = \frac{|qa+qc|}{2m\Delta V},$$

where qa, qc, m, and ΔV represent the anodic and cathodic charges on each scan, mass of the active material, and potential window of the cyclic voltammetry respectively. To compare the potential capacitances of the CE and activated carbon, the charge–discharge test was also carried out at a constant current density of 5.0 mA/cm^2 using a cycler (Toscat3000, Toyo Systems)

3. RESULTS AND DISCUSSION

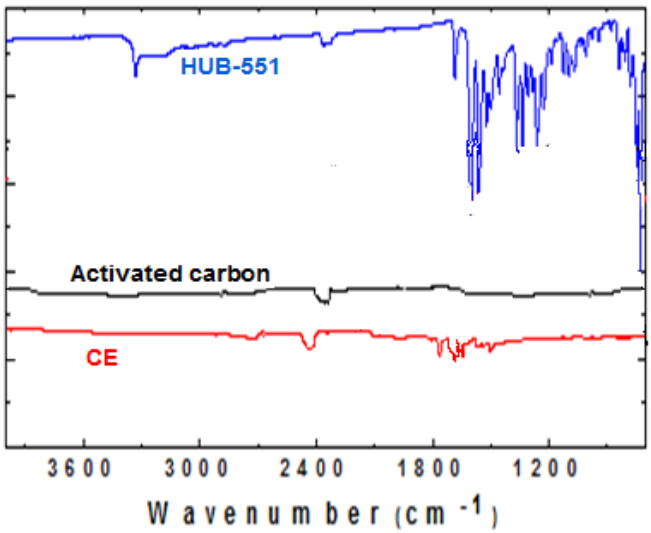

Figure 1. Fourier-transform infrared spectra of the synthesized HBU-551, the pristine activated carbon and the composite powder (2.5:7 w/w).

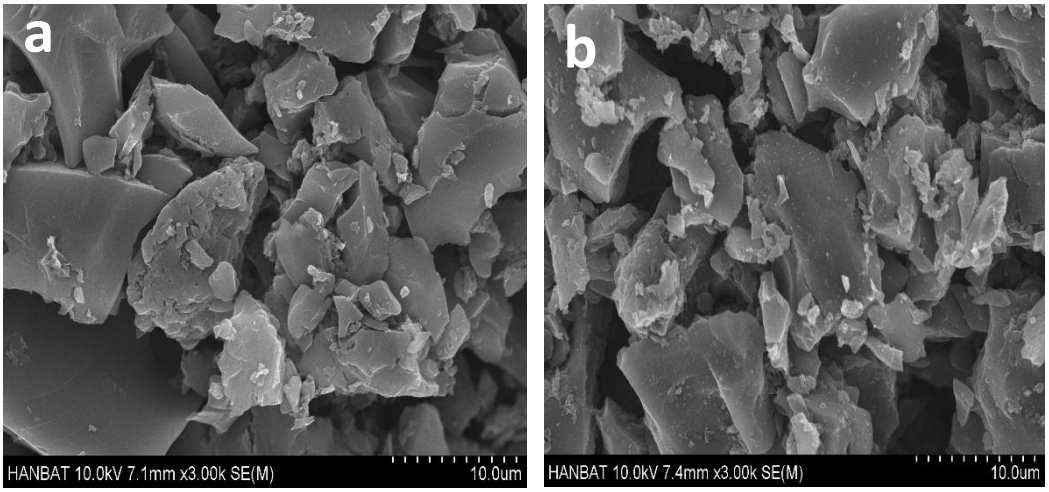

Figure 2. Surface morphologies of the (a) activated carbon, (b) HBU-551 CE

The Fourier-transform infrared spectrum in Fig. 1 confirms the chemical species on the surfaces of the sample powders including the HBU-551. In the HBU-551 powder, a characteristic absorption peak at about 1600 cm^{-1} band corresponds to C=O stretching vibration of quinone groups [18], which is expected to be involved in the redox reactions of 2,3-dihydro-1,4-naphthoquinone – 1,4-dihydroxynaphthalene couple. The peak at about 3400 cm^{-1} also seems to correspond to the stretching vibration of amino groups (—NH—) in the skeleton of HBU-551. However, activated carbon powder (MSC-30) shows no distinct infrared spectrum band over the entire wave number range. Meanwhile, the composite powder including the HBU-551 exhibited slight traces of the C=O stretching vibration of quinone group and the —NH— in the skeleton of HBU-551. That is, the CE composing of activated carbon and the HBU-551 (7:2.5 w/w) may be expected to exhibit a combined effect of activated carbon and the HBU-551 on the electrochemical performance of the electrodes.

The morphological property of the CE is investigated using Force emission scanning electron microscope. Fig 2a and 2b shows the micrographs of the activated carbon and the CE respectively. From the micrographs of the CE, the organic powder blended perfectly with the activated carbon, i.e. the organic powder coated the surfaces and partially filled the pores of the activated carbon.

The ionic conductivity of the aqueous electrolytes was calculated using the following equation: $\delta = \frac{t}{\mathrm{RbA}}$,

where δ is the conductivity, Rb is the bulk resistance (in ohms), t is the separation between the two electrodes (in cm) and A is the area of the electrode. Rb values were taken from the intercept of first semicircle at x-axis. As shown in Fig. 3, 1 M H_2SO_4 had the highest ionic conductivity followed by HCl, NH_4Cl and finally H_3PO_4. H_2SO_4, The HCl and NH_4Cl are strong electrolytes which are completely ionized when dissolved in water. On the other hand, H_3PO_4 is a weak electrolyte which is not completely ionized when dissolved in water.

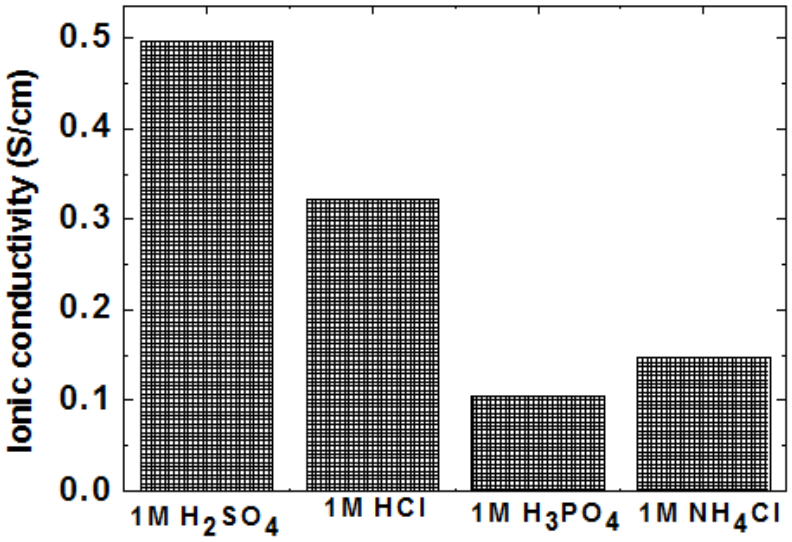

Figure 3. Ionic conductivity of the different electrolyte compared

Fig 4a shows the CVs for the pure organic powder without activated carbon in 1 M H_2SO_4 at a 100 mV/s and a potential range of -0.1~0.8 V vs. Ag/AgCl. The HBU-551 showed two pairs of redox peaks. More precisely, the pair of peaks at 0.18 V (anodic)/0.15 V (cathodic) corresponds to a 2, 3-dihydro-1, 4-naphthoquinone –1, 4-dihydroxynaphthalene couple redox transition (proposed mechanism is depicted 1c).

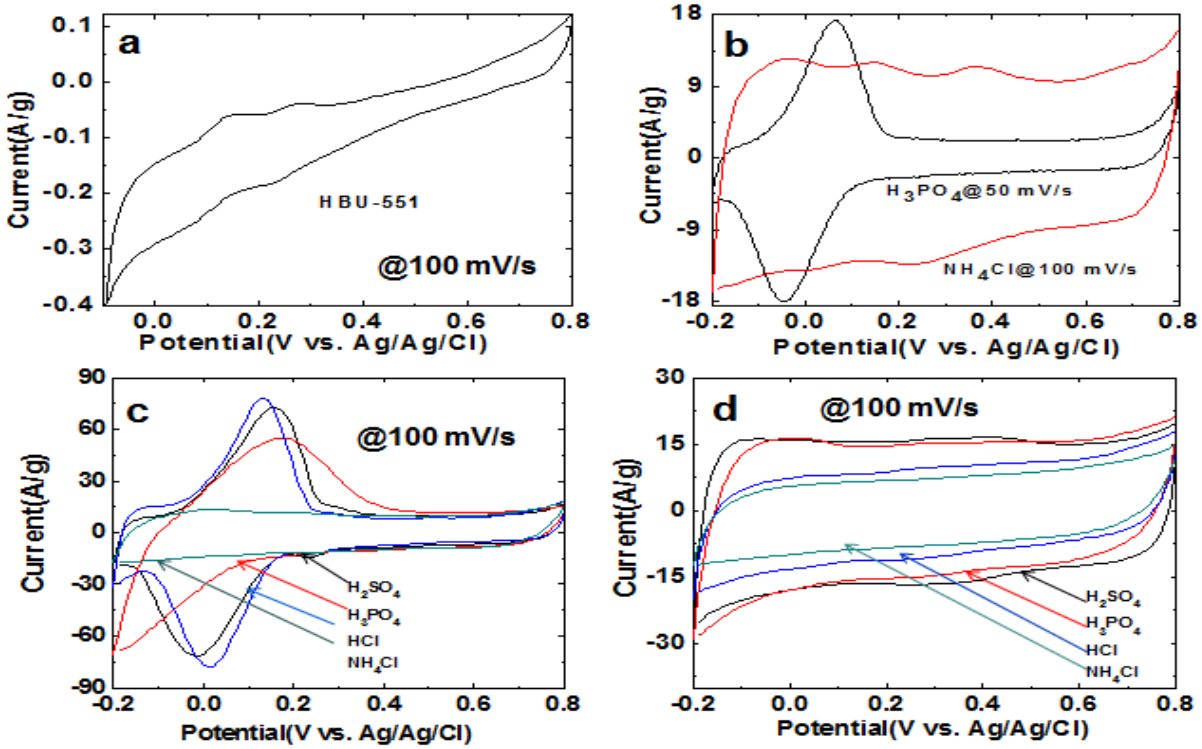

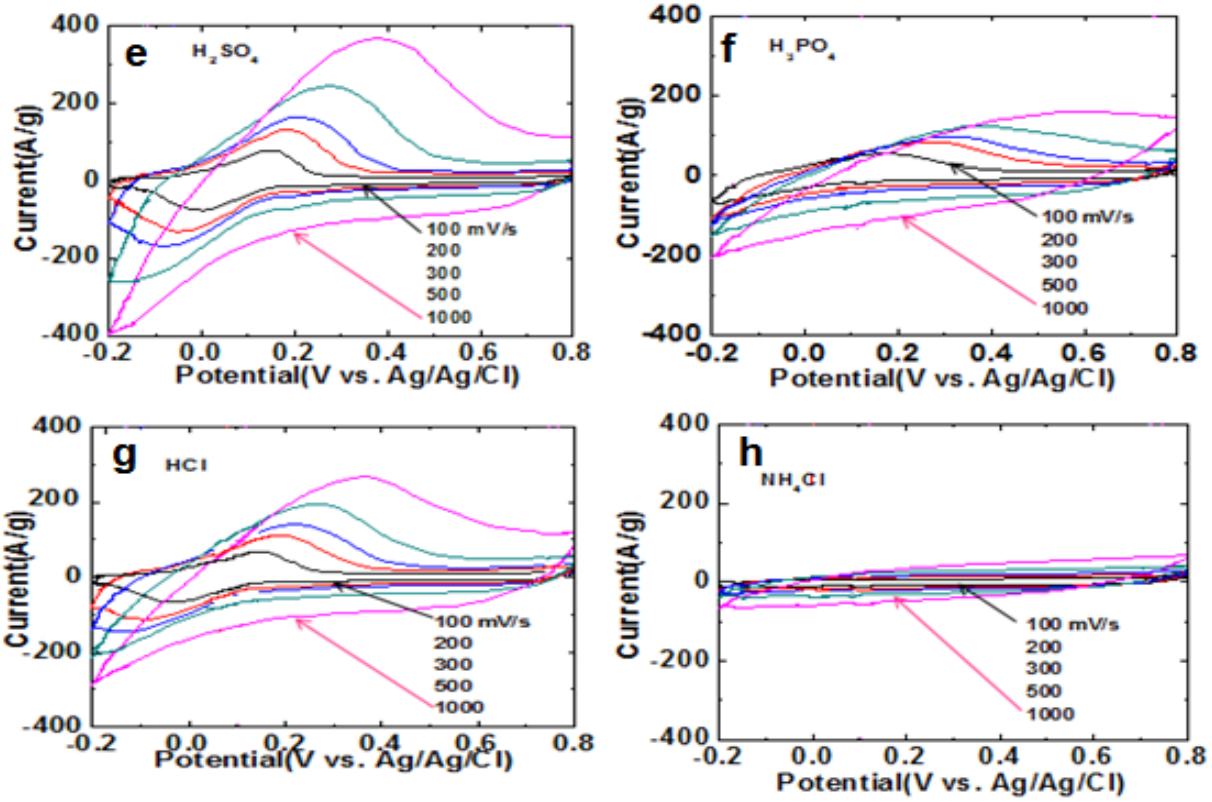

Figure 4. CVs of (a) pure HBU-551 in 1 M H_2SO_4 (b) electrode in NH_4Cl at 100 mV/s and in H_3PO_4 a t 50 mV/s (c) CE in different electrolyte (d) pristine activate carbon in different electrolyte and CE in (e) H_2SO_4 (f) H_3PO_4 (g) HCl (h) NH_4Cl at 100-1000 mV/s in 1 molar of the electrolytes

Again, the HBU-551 showed an extra pair of peaks corresponding to the redox of the —NH— groups in the indole structure [21] at 0.29 V (anodic)/0.25 V (cathodic). Fig. 4b shows the cyclic voltammograms of the activated carbon electrode measured at 100 mV s^{-1} in the different electrolytes. At that scan rate, the cyclic voltammogram of the activated carbon electrode in all the electrolytes exhibited a highly rectangular shape which is close to a typical electric-double-layer-capacitor behavior. The electrodes in H_2SO_4 and H_3PO_4 showed voltammograms with higher current density compared to the electrodes in HCl and NH_4Cl. However, the CE in all the electrolytes showed two pairs of redox peaks, corresponding to redox active reactions of the HBU-551 in all the electrolytes solution. The pair of peaks located at 0.15 V (anodic)/0.0 V (cathodic) corresponds to a 2, 3-dihydro-1,4-naphthoquinone –1,4-dihydroxynaphthalene redox transition, whereas the other pair of peaks at 0.25 V (anodic)/0.2 V (cathodic) may be matched with the redox of the —NH groups of the indole structures within the HBU-551. The redox behavior of —NH— groups also seems to be similar to the reversible redox process of nitrogen in the five-membered rings compounds such as in pyrrole structures [21-24]. Thus, the redox reaction of the HBU-551 occurs by a single-step three-electron ($3e^-$) and three-proton ($3H^+$) (see Fig.1c). The CE in H_2SO_4 and HCl demonstrated excellent reversible voltammograms compared to H_3PO_4 and NH_4Cl at 100 mV/s in agreement with their ionic conductivity. From the graphs, diffusion of hydrogen ions greatly influences the redox activity of the HBU-551 in the CE. The H_3PO_4 shows better and reversible voltammogram at lower scan rate than at higher scan rate (see Fig. 4b and 4c). This result may be attributed to the size of the ions due to incomplete ionization of the ions when dissolved in water. The CE in NH_4Cl showed tiny peaks at 0.18

V (anodic)/0.02 V (cathodic) which may corresponds to 2, 3-dihydro-1,4-naphthoquinone –1,4-dihydroxynaphthalene redox transition and the redox behavior of —NH— groups may be located around 0.4 V (anodic)/0.25 V (cathodic) (see Fig 4b). Furthermore, from Fig. 4c, the cyclic voltammograms of the CE in the H_2SO_4 and HCl electrolytes exhibited similar shapes with higher peak intensities, due to the high ionic conductivity (tendency to lose a proton (H^+) easily) and also over the entire scan rate range 100~1000 mV/s (See fig 4e and 4g). Over the same scan range, the CE in H_3PO_4 showed lower peak intensities compare to the strong acids and the CE showed little or no peaks in NH_4Cl over the entire scan rates (see Fig. 4f and 4h).

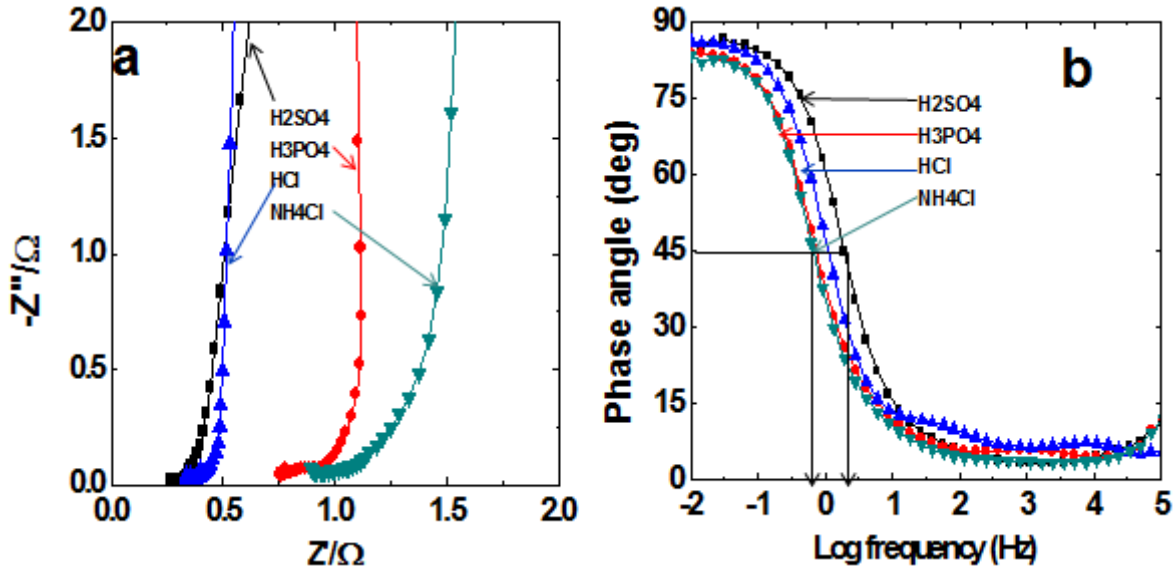

Figure 5. (a) Nyquist plots (b) Bode plot of the CE in 1 molar of the electrolytes in a frequency range of 10^{-2}~10^5Hz and at bias potential of 0.5 V

In order to assess the conductivities of the CE and their compatibility in the different electrolytes, the CE were subjected to complex impedance measurements at 25℃. The Nyquist plots are shown in Fig. 5a. From the plot, the CE in the different electrolyte contained small semicircles at high frequency and a small ~45◦ inclined line at middle frequency which is known as diffusive or Warburg resistance of ions with electrode [19] and imaginary parts of impedance at low frequency region are nearly linear. Comparing the resistive behaviors of the CE in each electrolyte, from the real axis (Z') intercept of the Nyquist plot, the CE in H_2SO_4 and HCl involves a lower resistivity and thereby a higher electrical conductivity than the CE in H_3PO_4 and NH_4Cl electrolytes. In all the electrolytes, the CE exhibited lower solution resistance than 1.5 Ω. The Bode is depicted in Fig. 5b, from the plots, the CE in the different electrolytes confirmed phase angle higher than 60 ^{o} until about 1.0 Hz. The frequency where Φ = -45 is identified as the capacitor response frequency (frequency response to ideal capacitor behavior) [20]. The CE in 1 M H_2SO_4 showed the fastest response time of 0.398 s (=1/ ($10^{2/5}$x10^0 Hz)) compared to NH_4Cl which recorded a slower response time of 1.514 s (=1/ ($10^{4.1/5}$x10^{-1} Hz)). The response times of the CE in HCl and H_3PO_4 falls between the response values of H_2SO_4 and NH_4Cl in agreement with their ionic conductivities.

Fig. 6a-b shows the high-rate capability of specific capacitances for the activated carbon and the CE in the different electrolytes. At the first cycle measured at low scan rate of 100 mV/s, higher specific capacitances are obtained: over 216 Fg^{-1}, 219 Fg^{-1}, 198 Fg^{-1} and 109 Fg^{-1} for the CE over 158 Fg^{-1}, 150 Fg^{-1}, 100 Fg^{-1} and 77 Fg^{-1} for the activated carbon electrode in 1M H_2SO_4, 1M H_3PO_4, 1M HCl and 1M NH_4Cl respectively.

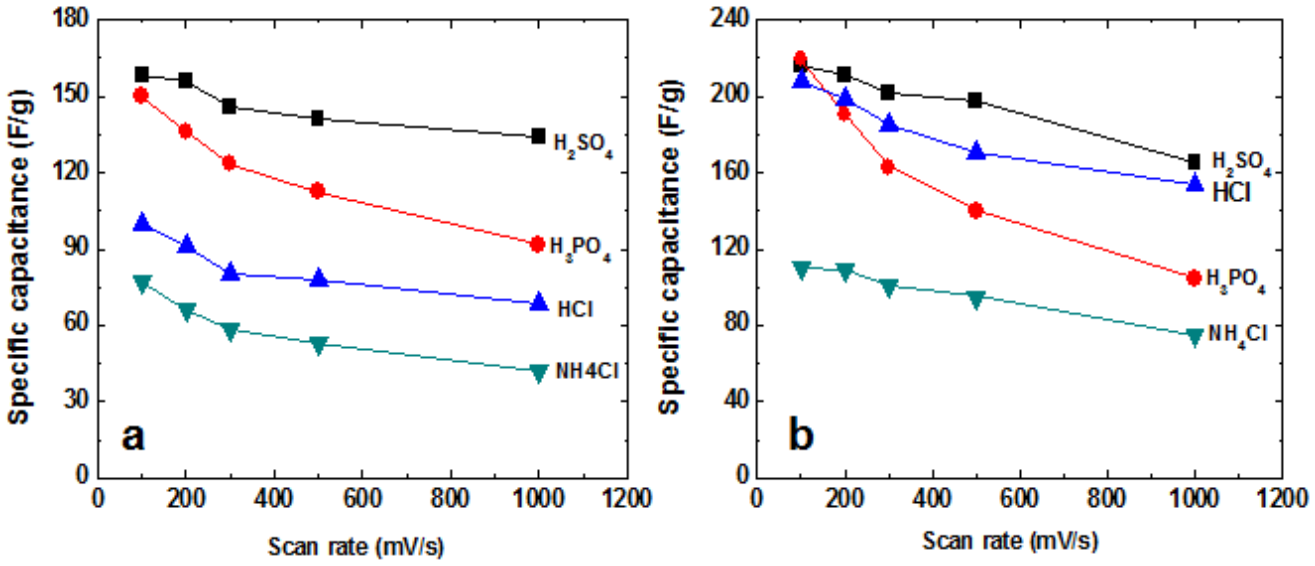

Figure 6. Specific capacitances of (a) pristine activated carbon (b) CE in the different electrolyte as a f unction of scan rate

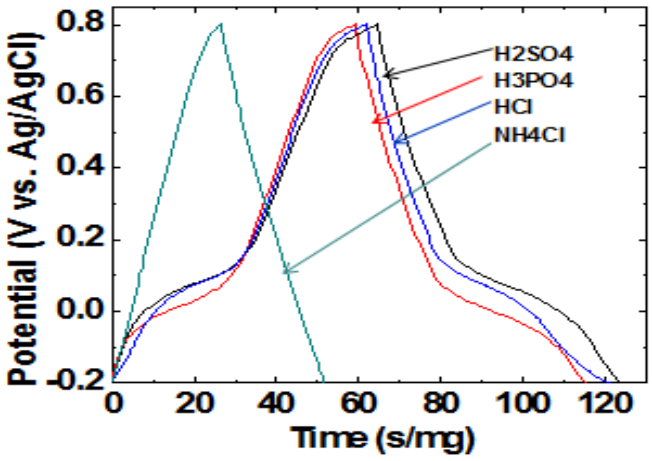

Figure 7. Charge–discharge profiles of the CE in the different electrolyte, measured at a current densit y of 5.0 mA cm^{-2} and a potential range of -0.2 – 0.8 V vs. Ag/AgCl in 1 molar of the electrolyte s

The difference in the specific capacitances between the activated carbon and the CE is due to the formation of pseudocapacitance by the redox reactions of the 2,3-dihydro-1,4-naphthoquinone –

1,4-dihydroxynaphthalene couple. In addition, the nitrogen species in the indole structure in the side groups of HBU-551 skeleton. At higher scan rate, the CE in H_3PO_4 shows a steep decreasing specific capacitance with increasing scan rate; this may be attributed to the poor mobility and the large size of the ion as a result of incomplete ionization of the acid. Both activated carbon and the CE in NH_4Cl showed lower specific capacitance. In consistence with scheme 1c, the electrochemical activity of HBU-551 is dependent on the number of protons. With more protons, (tendency to lose a proton (H^+) easily) the higher the capacitance contribution.

Fig. 7 shows the charge–discharge profiles of the CE, recorded at a constant current density of 5.0 mA cm^2. In this figure, all CE in the different electrolyte exhibited symmetric shapes. An average cycle time of the charge–discharge is in the order of H_2SO_4 > HCL > H_3PO_4 > NH_4Cl. Specifically, the CE in NH_4Cl electrolyte yielded the lowest charge-discharge average time of 52 s due to less amount of free hydrogen ions and hence low conductivity. On the other hand, H_2SO_4 yielded the highest average charge-discharge time of 125 s. The average charge-discharge time of the CE in HCl and H_3PO_4 are located between H_2SO_4 and NH_4Cl. Since the measurement is taken at a constant current, a longer cycle time means that a higher amount of electric energy is stored in the supercapacitor.

4. CONCLUSION

In this study, a CE consisting of activated carbon and quinine derivative (HBU-551) was synthesized chemically then probed in different hydrogen ion conducting electrolytes for a supercapacitor application. The electrolyte such as 1M H_2SO_4, 1M HCl, 1M H_3PO_4 and 1M NH_4Cl induce different electrochemical properties in the CE. The highest capacitance was obtained in 1M H_2SO_4 followed by HCl, H_3PO_4 and NH_4Cl in the scan rate range of 100-1000 mV/s. From the results, it may be concluded that the electrochemical activity of HBU-551 in the CE is dependent on the number of protons present in the electrolyte. The more proton the electrolyte can produce (tendency to lose proton (H^+) easily), the higher the capacitance contribution.

Reference

1. D. Bélanger, X. Ren, J. Davey, F. Uribe, S. Gottesfeld, *J. Electrochem. Soc.* 147 (2000) 2923–2929[2] B.C. Kim, J.S. Kwon, J.M. Ko, J.H. Park, C.O. Too, G.G. Wallace, *Synth. Metal* 160 (2010) 94–98
2. W. Jung Ha, M. Latifatu, J. Mi, L. H. Soo, K. B. Cheol, H. Louis, P. H. Jeong, K.M. Kwang, K.M Jang, *Synth. Metal* 203 (2015) 31–36
3. Kalinathan, K. DesRoches, D.P.; Liu, X.; Pickup, P.G. *J. Power Sources* 181 (2008) 182–185.
4. M. Yao, S. Yamazaki, H. Senoh, T. Sakai, T. Kiyobayashi, *Mat. Sci. Eng. B.* 177 (2012) 483–487.
5. Y. Hanyu, Y. Ganbe, I. Honma, *J. Power Sources* 221 (2013) 186–190.
6. W. Wang, W. Xu, L. Cosimbescu, D. Choi, L. Li, Z. Yang, *Chem. Commun.* 48 (2012) 6669–6671.
7. W. Choi, D. Harada, K. Oyaizu, H. Nishide, *J. Am. Chem. Soc.* 133 (2011) 19839–19843.
8. S. Suematsu, K. Naoi, *J. Power Sources* 97-98 (2001) 816–818
9. S. Panero, F. Ciuffa, A. D'Epifano, B. Scrosati, *Electrochim. Acta* 48 (2003) 2009-2014.
10. H. Yu, J. Wu, L. Fan, Y. Lin, K. Xu, Z. Tang, C. Cheng, S. Tang, J. Lin, M. Huang, Z. Lan, *Journal*

of Power Sources 198 (2012) 402– 407
11. L. Francesco and S. Pietro, *Electrochemical and Solid-State Letters*, 7 (11) (2004) A447-A450
12. A. Lewandowski, M. Zajder, E. Fra¸ckowiak, F. Be´guin, *Electrochimica Acta* 46 (2001) 2777–2780.
13. N. Gupta and H. Linschitz, *J. Am.Chem. Soc.* 1997, 119, 6384-6391.
14. P. S. Guin, S. Das and P. C. Mandal, *Int. J. Electrochem. Sci*., 3 (2008)1016 - 1028
15. F. C. Anson and B. Epstein, *J. Electrochem. Soc.*115 (1968) 1155–1158
16. P. He, R. M. Crooks, and L. R. Faulkner, *J. Phys. Chem.* 94 (1990) 1135-1141
17. S.T. Senthilkumar, R.K. Selvan, N. Ponpandian, J.S. Melo, *RSC Adv.* 2 (2012) 8937–8940
18. H. Zheng, T. Zhai, M. Yu, S. Xie, C. Liang, W. Zhao, Z. Zhang, X. Lu, *J. Mater. Chem.C*,1 (2013) 225-229
19. W. Sugimoto, H. Iwata, K. Yokoshima, Y. Murakami, and Y. Takasu, *J. Phys. Chem. B* 109 (2005) 7330-7338.
20. S. Roldán, Z. González, C. Blanco, M. Granda, R. Menéndez, R. Santamaría, *Electrochim. Acta* 56 (2011) 3401–3405.
21. A.M. Bond, F. Marken, E. Hill, R.G. Compton, H. Hügel, *J. Chem. Soc. Perkin Trans.* 2 (1997) 1735–1742.
22. M. Díaz-González, C. Fernández-Sánchez, A. Costa-García, *Electroanalysis* 14 (2002) 665–670.
23. P. Fanjul-Bolado, D. Hernández-Santos, P.J. Lamas-Ardisana, A. Martín-Pernía, A. Costa-García, *Electrochim. Acta* 53 (2008) 3635–3642.